• Basic Research •

# A Trojan horse biomimetic delivery system using mesenchymal stem cells for HIF-1α siRNA-loaded nanoparticles on retinal pigment epithelial cells under hypoxia environment

*Lei Zhang[1], Jie-Jing Yan[2,3], Hai-Yan Wang[1], Mu-Qiong Li[4], Xi-Xi Wang[5], Li Fan[4], Yu-Sheng Wang[2]*

[1]Shaanxi Eye Hospital, Xi'an People's Hospital (Xi'an Fourth Hospital), Xi'an 710004, Shaanxi Province, China
[2]Department of Ophthalmology, Xijing Hospital, Xi'an 710032, Shaanxi Province, China
[3]Ophthalmology Department, Xi'an No.1 Hospital, the First Affiliated Hospital of Northwest University, Xi'an 710002, Shaanxi Province, China
[4]Department of Pharmaceutical Chemistry and Analysis School of Pharmacy Air Force Medical University, Xi'an 710032, Shaanxi Province, China
[5]Department of Mathematics and Statistics, University of Arkansas at Little Rock, Little Rock, AR 72204, USA
**Co-first authors:** Lei Zhang and Jie-Jing Yan
**Correspondence to:** Hai-Yan Wang. Shaanxi Eye Hospital, Xi'an People's Hospital (Xi'an Fourth Hospital), Xi'an 710004, Shaanxi Province, China. whyeye@126.com; Yu-Sheng Wang. Department of Ophthalmology, Xijing Hospital, Xi'an 710032, Shaanxi Province, China. wangys003@126.com
Received: 2022-04-28 Accepted: 2022-09-15

## Abstract

● **AIM:** To demonstrate the feasibility of mesenchymal stem cell (MSC)-mediated nano drug delivery, which was characterized by the "Trojan horse"-like transport of hypoxia-inducible factor-1α small interfering RNA (HIF-1α siRNA) between MSCs and retinal pigment epithelial cells (RPE) under hypoxia environment.

● **METHODS:** Plasmid and lentivirus targeting the human HIF-1α gene were designed and constructed. HIF-1α siRNA was encapsulated into poly(lactic-co-glycolic acid) nanoparticles (PLGA-NPs) through the water-in-oil-in-water (w/o/w) multiple emulsion technique. The effect of PLGA-NPs uptake on the expression of HIF-1α mRNA was tested in RPE cells by real-time quantitative polymerase chain reaction (qPCR) and additional transfected conditions were used as control, including lentivirus group, nude plasmid group and blank PLGA group. MSCs were transfected with the NPs and the transfection efficacy was evaluated by flow cytometry. Transwell co-culture system of transfected MSCs and RPE cells was constructed under hypoxia environment. The effects of MSC-loaded HIF-1α siRNA PLGA-NPs on proliferation, apoptosis, and migration of RPE cells were then evaluated. The effect of transfected MSCs on HIF-1α expression of RPE cells was analyzed by using qPCR at the time points 24h, 3d, and 7d.

● **RESULTS:** The average diameter of PLGA-NPs loaded with HIF siRNA was 314.1 nm and the zeta potential was -0.36 mV. The transfection efficiency of PLGA-NPs was 67.3%±5.2% into MSCs by using flow cytometry. Compared with the lentivirus group, the PLGA-NPs loaded with HIF-1α siRNA can effectively reduce the expression of HIF-1α mRNA up to 7d in RPE (0.63±0.05 at 7d, $P$<0.001). In the Transwell co-culture system of transfected MSCs and RPE, the abilities of proliferation (2.34±0.17, 2.40±0.28, 2.47±0.24 at 48h, $F$=0.23, $P$=0.80), apoptosis (14.83%±2.43%, 12.94%±2.19%, 12.39%±3.21%; $F$=0.70, $P$=0.53) and migration (124.5±7.78, 119.5±5.32, 130±9.89, $F$=1.33, $P$=0.33) of the RPE cells had no differences between MSC-loaded HIF-1α siRNA PLGA-NPs and other groups. The inhibition of PLGA on the HIF-1α mRNA expression in RPE cells could continue until the 7$^{th}$ day, the level of HIF-1α mRNA was lower than that of other groups ($F$=171.98, $P$<0.001).

● **CONCLUSION:** The delivery of PLGA-NPs loaded with HIF-1α siRNA carried by MSCs is found to be beneficial temporally for HIF-1α mRNA inhibition in RPE cells under hypoxia environment. The MSC-based bio-mimetic delivery of HIF-1α siRNA nanoparticles is a potential method for therapy against choroidal neovascularization.

● **KEYWORDS:** hypoxia; mesenchymal stem cells; poly(lactic-co-glycolic acid) nanoparticles; hypoxia-inducible factor-1α; retinal pigment epithelial cells

**DOI:10.18240/ijo.2022.11.03**

**Citation:** Zhang L, Yan JJ, Wang HY, Li MQ, Wang XX, Fan L, Wang YS. A Trojan horse biomimetic delivery system using mesenchymal stem cells for HIF-1α siRNA-loaded nanoparticles

on retinal pigment epithelial cells under hypoxia environment. *Int J Ophthalmol* 2022;15(11):1743-1751

## INTRODUCTION

Choroidal neovascularization (CNV) is a significant cause of vision loss in all age groups. Anti-vascular endothelial growth factor (VEGF) drug can effectively treat neovascularization in most, but not all patients and there are safety concerns about its' intrinsic defect and long-term effects[1]. Therefore, better therapeutic agents are needed to study for the effective treatment of this vision-threatening lesion[2]. It has long been known that hypoxia plays a central role in pathogenesis of CNV. In response to hypoxia, the hypoxia-inducible factor-1 (HIF-1) mediates the transcription of several target genes, including VEGF. Compared with anti-VEGF, inhibition of HIF-1 activity can simultaneously reduce a variety of downstream multiple proangiogenic factors[3-5].

RNA interference (RNAi) is a promising gene knockdown strategy that employs small interfering RNA (siRNA) for silencing specific gene expression[6]. Nonetheless, there remain number challenges *in vivo* siRNA delivery such as the renal clearance and the inability of RNA to pass through the cell membrane[7]. Mesenchymal stem cells (MSCs) have high chemotaxis to the hypoxic microenvironment, and it has been shown that the hypoxic preconditioning increases the migration and homing of MSCs[8]. The use of stem cells as cellular vectors for drug-loaded nanoparticles seems to be a highly promising approach to targeting tissues[9]. In previous study, we found that MSCs also had the specific ability of migrate to the lesion site of CNV, and human pigment epithelial-derived factor (PEDF) production by adenoviral (Ad) PEDF/MSCs *in vitro*[10]. Our goal is to find a safer and longer-term method of using HIF-1α siRNA loaded in MSCs to reach the CNV site to inhibit the angiogenesis.

Poly(lactic-co-glycolic acid) (PLGA) is a Food and Drug Administration (FDA) approved polymer with great biodegradability, biocompatibility, and excellent ocular safety for local use. A clinic trial of PLGA-based intravitreal (IVT) injectable formulation of sunitinib malate for the patients of neovascular age-related macular degeneration (AMD) is ongoing (NCT03249740)[11]. Our previous study showed PLGA nanoparticles (NPs) loaded with HIF-1α short hairpin RNA could transfer specific pDNA and inhibit the formation of experimental CNV in a laser-induced rat model by IVT administered[12]. However, the risks of retinal detachment and endophthalmitis will increase with frequent IVT injection as well as retina toxicity had to be concerned. A biodegradable nanoparticulate system consisting of PLGA was synthesized to be loaded with a HIF-1α siRNA agent, which was subsequently engulfed by MSCs, forming an MSC-based biomimetic delivery system (MSC-PLGA-HIF-1α siRNA). Therefore, by this delivery system, therapeutics can be efficiently delivered to CNV region by a so-called Trojan horse strategy[13].

## MATERIALS AND METHODS

**Ethical Approval** This research was approved by Xi'an People's Hospital (Xi'an Fourth Hospital) Clinical Research Ethics Committee (No.20200037), which was adhered to the tenets of the Declaration of Helsinki.

**Cell Culture of ARPE-19** ARPE-19 cell line (American Type Culture Collections, Manassas, VA, USA, passage 4) were maintained and passaged 5-10 in standard culture dishes.

**Isolation and Culture of Human Mesenchymal Stem Cells** The human mesenchymal stem cells (hMSCs) were obtained by heparinized human bone marrow from bone fragments in patients with fracture. Bone mononuclear cells were isolated by Percoll density gradient centrifugation (below 1.073 g/mL, Sigma, USA). Cells were cultured in Dulbecco's modified Eagle's medium-low glucose (DMEM-LG, Hyclone, USA) supplemented with 10% fetal bovine serum (FBS; Hyclone, USA), and maintained at 37□ in 5% $CO_2$. Non-adhered cells were removed by washing in 48h, and adherent cells were cultured with the medium being replaced every 3d. After the cells were 80%-90% confluent, the cells were detached with 0.25% trypsin and then seeded at 1:3 in a flask, being used either for gene transfection or for further culture and passage 3-4. hMSCs were checked for multi-linage differentiation by adipogenic and osteogenic differentiation assays. Briefly, osteogenesis was induced by culturing MSC monolayer in medium containing $10^{-8}$ mol/L dexamethasone, 10 mmol/L β-glycerol phosphate, and 50 mg/L ascorbic acid 2-phosphate. Calcium deposition was shown by Alzarin red staining. Adipogenesis was induced by using the induction medium including high-glucose DMEM, $10^{-6}$ mol/L dexamethasone, 100 μg/mL indomethacin, 10 μg/mL insulin, and 0.5 mmol/L 3-isobutyl-1-methylxanthine. Induction was confirmed by oil red O staining.

**Preparation of HIF siRNA-loaded PLGA Nanoparticles** HIF-1α siRNA was designed, constructed, and purified by Shanghai Genechem Co., LTD (Shanghai, China). The antisense sequence of siRNA targeting HIF-1α was 5'-CCG GCGTTGTGAGTGGTATTATTCTCGAGAATAATACCAC TCACAACGTTTTTG-3'. The nanoparticles were prepared by a double emulsion solvent evaporation technique (w/o/w). Briefly, poly(lactide-co-glycolide) with acid end groups was dissolved in 1.5 mL of dichloromethane (DCM). The 100 μg HIF-1α siRNA plasmid lyophilized powder was dissolved in Tris-EDTA buffer solution to a final pH7.8. The solutions were mixed and emulsified using a high-speed agitator to obtain primary emulsion (w/o). The primary emulsion was added into a 10 mL 1% solution of polyvinyl alcohol (PVA) using a

high speed agitator (24 000 rpm, 6min). The double emulsion was added into 30 mL 1% PVA solution and stirred it in the fume hood overnight. After centrifugation for 20min (4□, 13 000 rpm), the precipitates were collected and washed with deionized water for three times to remove free genes and PVA. The freeze-dried nanoparticles were stored at 4□.

**Characterization of Nanoparticles** For size measurement, the nanoparticles were resuspended in purified deionized water. The microscopic morphology was observed by scanning electron microscopy; the particle size and Zeta potential were measured by Malvem laser particle size analyzer.

***In Vitro* Transfection** Lentivirus or PLGA (γ-ray irradiation sterilization) was diluted with the DMEM culture medium. Cells were cultured in 24-well plates and transfected with lentivirus at multiplicity of infection (MOI) =100 or PLGA NPs encapsulating siRNA. The siRNA concentration was constant at 100 nmol/L per well. Then 48-72h after transfection, the medium was replaced with fresh DMEM culture medium and transfected hMSCs were used in the following co-culture cell model studies.

**Cellular Uptake of PLGA Nanoparticles** The cells grow on cover glass for 72h. Then the coverslips were taken out and rinsed with phosphate balanced solution (PBS) twice. The adhesive cells were fixed for 30min in 4% polyoxymethylene in PBS at 4□. Then the samples were covered with 50% glycerol (v/v) and green fluorescent protein (GFP) was observed under an inverted fluorescence microscope. The cells were enzymatically lifted from culture flasks and re-suspended with media at a density of $1\times10^6$ cells/mL. Then GFP-positive cells were detected by using flow cytometry.

**Detection of HIF-1α mRNA in Retinal Pigment Epithelial Cells by Real-time Quantitative PCR** RNA extraction was performed using Trizol (Invitrogen, USA) according to the manufacturer's instructions. Total RNA (1 mg) was reverse transcribed according to the manufacturer's protocol (Invitrogen, USA). PCR reactions were performed using real-time 7500 under the following conditions: 95□ for 10min followed by 40 cycles of 10s of denaturation at 95□, and 30s of extension at 60□. The primer sequences were as follows: GAPDH-F: 5'-GCTGAGTACGTCGGTGGAG-3'; GAPDH-R: 5'-CAGTTGGTGGTCAGGAGG-3'; The amplified fragment was 158 bp; HIF-1α-F: 5'-TCGGCGAAGTAAATCTGAA-3'; HIF-1α-R: 5'-CAAATCACCAGATCCAGAAG-3'; The amplified fragment was 151 bp.

**Establishment of Hypoxia Model and Co-culture Cell Model** Hypoxic model was established in a 5% $O_2$ and 5% $CO_2$ hypoxic cell incubator at 37□. Co-culture cell model was established by using Transwell (pore size 0.4 μm). RPE cells were placed in the lower layer (24-well culture plates) and hMSCs were placed in the upper layer (chamber). The cell density was $1\times10^4$ cells/mL, and a 200 μL volume was seeded.

**Trans-well Cell Proliferation, Migration, and Apoptosis Assays** Cell proliferation was determined using Trans-well chambers with 0.4-μm sized pores (Corning Costar, Cambridge, UK). RPE cells (2000 cells/0.2 mL) were placed in the upper chambers of each insert cultured in HG medium supplemented with 1% FBS, whereas hMSCs (2000 cells/0.2 mL) were placed in the lower chambers. After of incubation under hypoxia conditions (5% $O_2$), 10% cell counting kit-8 (CCK-8) solution was added at 12, 24, and 48h, in accordance with the manufacturer's instructions. The supernatants were transferred into 96 well plates and the absorbance value (optical density; OD) of each well was measured at 450 nm after incubation at 37□ for 3h.

Cell migration was determined using Trans-well chambers with 8-μm sized pores (Corning Costar, Cambridge, UK). RPE cells (2000 cells/0.2 mL) were placed in the upper chambers of each insert cultured in HG medium supplemented with 1% FBS, whereas hMSCs (2000 cells/0.2 mL) were placed in the lower chambers. After 24h of incubation under hypoxia conditions (5% $O_2$), the inserts were removed. Cells that have migrated the bottom of the Transwell membrane were stained with 0.1% crystal violet. Six representative fields of each Trans-well were captured using a microscopy (Optika, Ponteranica, Italy). The migrated cells were counted in six randomly selected fields.

Cell apoptosis was determined using Trans-well chambers with 0.4-μm sized pores (Corning Costar, Cambridge, UK). hMSCs (2000 cells/0.2 mL) were placed in the upper chambers of each insert cultured in HG medium supplemented with 1% FBS, whereas RPE cells (2000 cells/0.2 mL) were placed in the lower chambers. After 24h of incubation under hypoxia conditions (5% $O_2$), apoptotic effects were tested on RPE cells using flow cytometer (Accuri BD C6, USA) by Annexin V-FITC/PI.

**Statistical Analysis** All data were expressed as mean±standard deviation (SD) and analyzed by one-way analysis of variance (ANOVA) followed by contrast analysis (LSD *t*-test when equal variances assumed, and Dunnett's T3 test when equal variances not assumed) using the IBM SPSS Statistics version 26 (IBM SPSS Inc., Chicago, USA). A *P* value of less than 0.05 was considered statistically significant.

## RESULTS

**Characterization of Hypoxia-Inducible Factor siRNA Loaded PLGA Nanoparticles** The HIF siRNA-loaded PLGA NPs prepared in this study were in round shape and with an average diameter of 314.1±16.4 nm (Figure 1). These NPs when dispersed in distilled water had a zeta potential of -0.36 mV (Figure 2). The scanning electron microscope (SEM) result showed that NPs were round shape and with an average diameter of 300 nm (Figure 3).

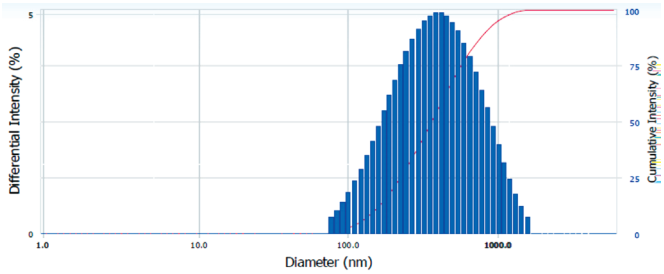


**Figure 1 Particle size distribution of PLGA loaded with HIF-1α siRNA (nanoparticles diameter 302.4 nm)** PLGA: Poly(lactic-co-glycolic acid); HIF-1α: Hypoxia-inducible factor-1α.

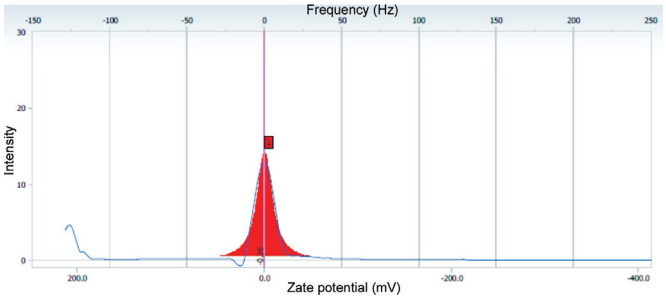


**Figure 2 The zeta potential distribution of the nanoparticles.**

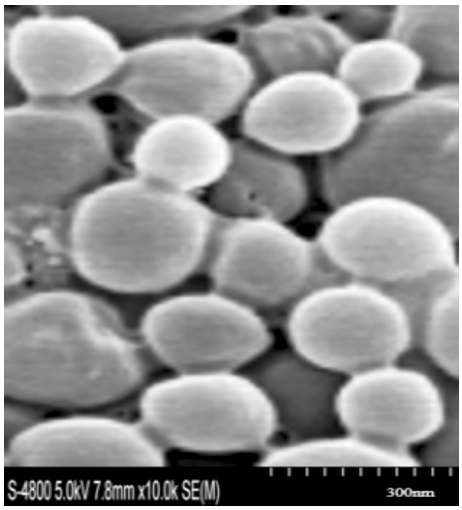


**Figure 3 The scanning electron microscope (SEM) of PLGA loaded with HIF-1α siRNA** Bar=300 nm. PLGA: Poly(lactic-co-glycolic acid); HIF-1α: Hypoxia-inducible factor-1α.

**Isolation and Culture of Human Mesenchymal Stem Cells** After 24h culture, irregular round or polygonal cells were observed, which were primary hMSCs (P0). After 1-3d primary culture, individual colonies were formed. Fourteen days later, 90% confluence of cells was visualized, and then the cells were trypsinized and passaged. After passaging, the cells grew in a uniform spindle and whirlpool shape. The individual cultured MSCs had osteogenic and adipogenic potential. On the 19$^{th}$ day of osteoblast induction, the cultured MSCs formed calcium nodules (Figure 4B). On the 7$^{th}$ day of adipoblast induction, lipid droplets were observed in the cytoplasm of MSCs (Figure 4C). In the control group, the cells grew densely and overlapped without calcium nodules or lipid droplets (Figure 4A). The flow cytometry analysis of cell surface markers showed: CD29+, CD34-, CD45-. The above results confirmed that they were MSCs (Figure 4D).

**Uptake of PLGA Nanoparticles Loaded-HIF siRNA** After 48h of transfection, GFP green fluorescence could be seen around the nucleus of hMSCs (Figure 5). And the transfection efficiency was (67.3±5.2)% by using flow cytometry (Figure 6).

**Effect of PLGA Nanoparticles Uptake on the Expression of HIF-1α mRNA in Retinal Pigment Epithelial Cells** All samples were divided in five groups, which were control group (without any treatment), lentivirus group (transfected with lentivirus with HIF-1α siRNA), nude plasmid group (transfected with empty plasmid), blank PLGA group (transfected with empty PLGA nanoparticles), and PLGA+siRNA group (transfected with nanoparticles loaded with HIF-1α siRNA). The expression of HIF-1α mRNA in RPE cells were detected at 24h, 3d, and 7d under hypoxic model. It was showed that HIF-1α mRNA in lentivirus group was significantly lower than that in the other four groups at 24h (0.49±0.06, $F$=37.71, $P$<0.001). The expression of HIF-1α mRNA in PLGA+siRNA group was significantly lower than that in the control group, nude plasmid group and blank PLGA group at 24h, 3d, and 7d ($P$<0.05). Compared with the lentivirus group, there were differences at 3d and 7d (lentivirus group 0.84±0.06 *vs* PLGA+siRNA group 0.57±0.04 at 3d, $P$=0.01; lentivirus group 1.13±0.10 *vs* PLGA+siRNA group 0.63±0.05 at 7d, $P$<0.001; Figure 7).

**Effect of Mesenchymal Stem Cells Loaded with HIF-1α siRNA Nanoparticles on Proliferation, Migration, and Apoptosis of Retinal Pigment Epithelial Cells in Hypoxia Model** There were three groups divided in this section, which were RPE group (only RPE cells were cultured in hypoxia model); co-culture group (RPE cells were co-cultured with MSCs in hypoxia model); PLGA+siRNA and co-culture group (RPE cells were co-cultured with MSCs loaded with HIF-1α siRNA NPs in hypoxia model).

The CCK-8 test results revealed that the proliferation increased in all groups at 12, 24, and 48h, but there was no difference among three groups at the same time points (1.70±0.17, 1.78±0.19, 1.80±0.14 at 12h, $F$=0.30, $P$=0.75; 1.93±0.19, 2.03±0.24, 2.12±0.24 at 24h, $F$=0.54, $P$=0.61; 2.34±0.17, 2.40±0.28, 2.47±0.24 at 48h, $F$=0.23, $P$=0.80; Figure 8). There was no significant difference in apoptosis among the three groups at 24h by flow cytometry (14.83%±2.43%, 12.94%±2.19%, 12.39%±3.21%, $F$=0.70, $P$=0.53; Figure 9). Trans-well results showed that there was no difference in the number of RPE migrating cells among the three groups at 24h (124.5±7.78, 119.5±5.32, 130±9.89, $F$=1.33, $P$=0.33; Figure 10).

**Effect of Mesenchymal Stem Cells Loaded with HIF-1α siRNA Nanoparticles on the Expression of HIF-1α mRNA**

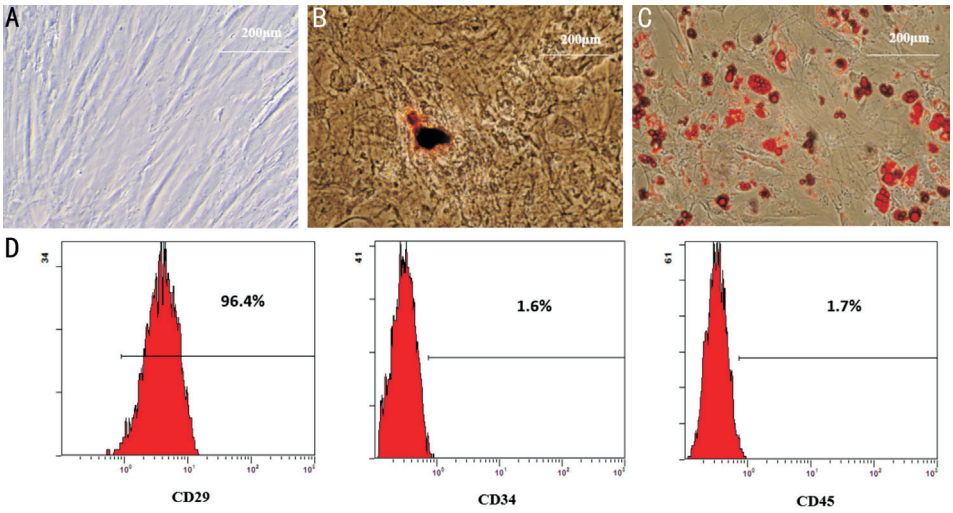


**Figure 4 The third passage of human mesenchymal stem cells showed uniform spindle growth (A) and after differentiation along the osteogenic (B, Alkaline red staining) and adipogenic pathways (C, oil red O staining). The positive rates of CD29, CD34 and CD45 were 96.4%, 1.6% and 1.7%, respectively (D, the flow cytometry analysis)** Bar=200 μm.

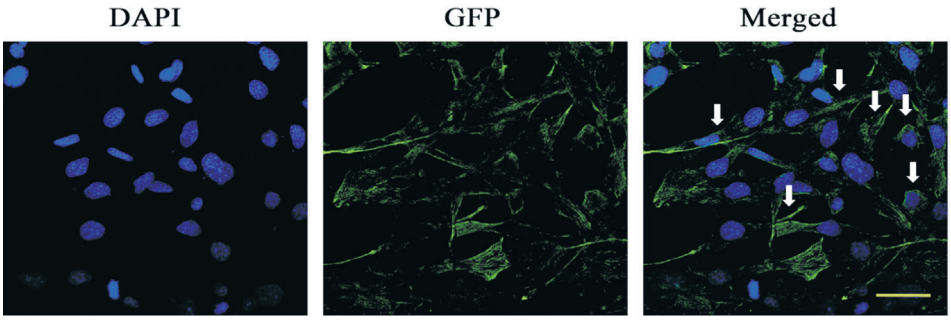


**Figure 5 Uptake of HIF-1α siRNA-loaded PLGA nanoparticles** DAPI in blue, GFP in green, and nanoparticles in cells indicated by arrow; bar=100 μm. PLGA: Poly(lactic-co-glycolic acid); HIF-1α: Hypoxia-inducible factor-1α; GFP: Green fluorescent proteins.

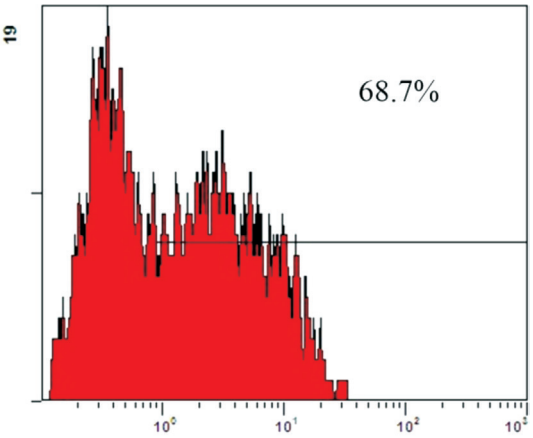


**Figure 6 The transfection efficiency of HIF siRNA loaded in PLGA nanoparticles** *n*=5. PLGA: Poly(lactic-co-glycolic acid); HIF-1α: Hypoxia-inducible factor-1α.

**of Retinal Pigment Epithelial Cells in Hypoxia Model** The expression of HIF-1α mRNA in RPE cells was detected at 24h, 3, and 7d. The results showed that the expression of HIF-1α mRNA in RPE cells co-cultured with MSCs loaded with HIF-1α siRNA NPs was significantly lower than that in RPE group and co-culture group at each time point (0.61±0.01, 1.49±0.07,

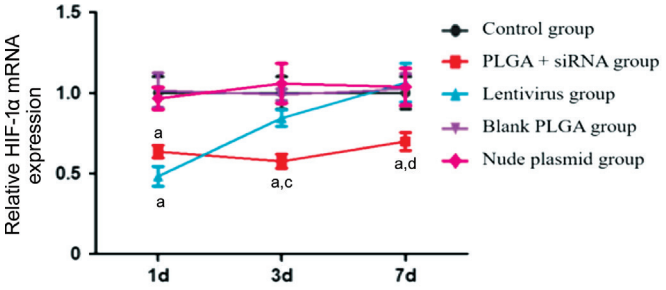


**Figure 7 The relative expression of HIF-1α mRNA in retinal pigment epithelial cells** $^{a}P<0.05$ *vs* control group; $^{c}P<0.05$, $^{d}P<0.001$ *vs* lentivirus group; *n*=3. PLGA: Poly(lactic-co-glycolic acid); HIF-1α: Hypoxia-inducible factor-1α.

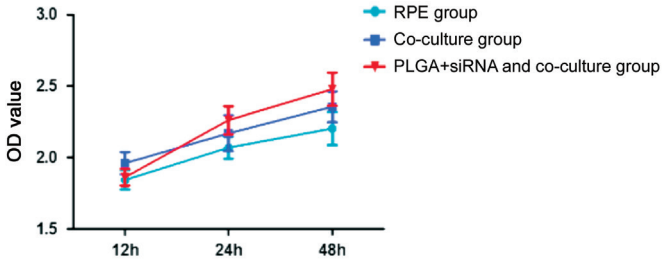


**Figure 8 The growth curve of RPEs by different culture methods in hypoxia model** *P*>0.05, *n*=3. PLGA: Poly(lactic-co-glycolic acid); RPE: Retinal pigment epithelial cells.

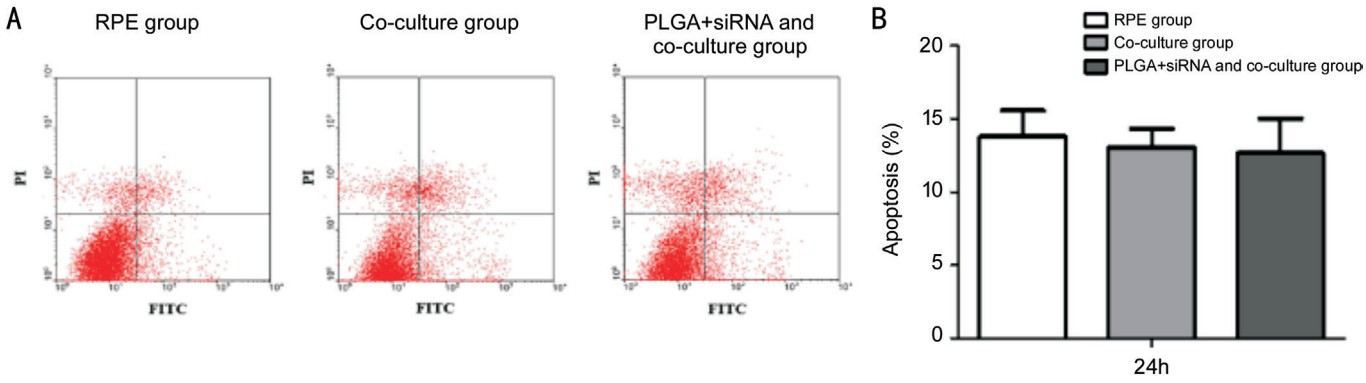


**Figure 9 The apoptosis of RPEs by different culture methods in hypoxia model for 24h** $P>0.05$, $n=3$. PLGA: Poly(lactic-co-glycolic acid); RPE: Retinal pigment epithelial cells.

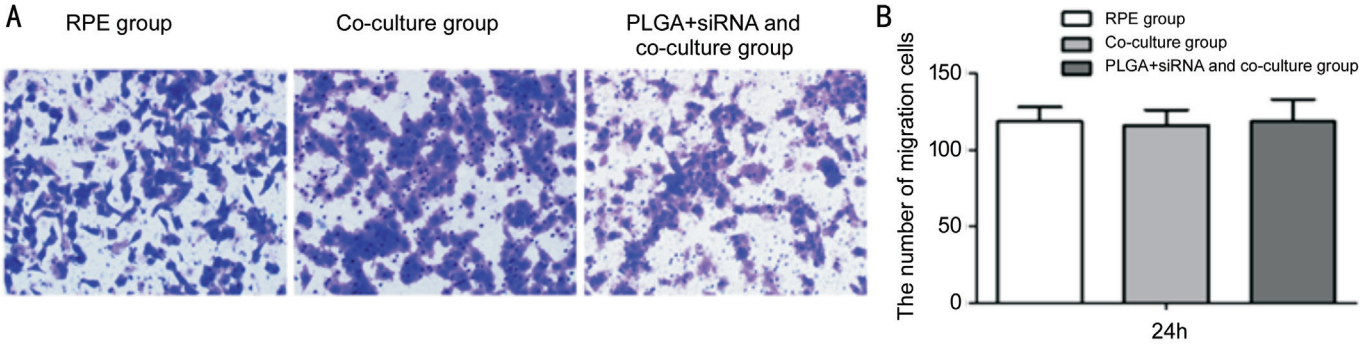


**Figure 10 The migration of RPEs by different culture methods in hypoxia model for 24h** $P>0.05$, $n=3$. PLGA: Poly(lactic-co-glycolic acid); RPE: Retinal pigment epithelial cells.

1.50±0.06 at 1d, $F=273.24$, $P<0.001$; 0.57±0.02, 1.51±0.05, 1.44±0.07 at 3d, $F=316.42$, $P<0.001$; 0.75±0.03, 1.28±0.02, 1.28±0.06 at 7d, $F=171.98$, $P<0.001$; Figure 11).

## DISCUSSION

Specifically targeting HIF transcription factors have been an attractive strategy for co-regulating many downstream angiogenic factors. In our previous study, we developed intravitreal administered HIF-1α short hairpin RNA loaded in PLGA NPs which can inhibit the formation of experimental CNV[12]. However, there are still surgical risks in intravitreal injection and underlying retina toxicity, and it is necessary to find appropriate siRNA delivery methods to reduce adverse reactions and target CNV lesion precisely. We previously found that MSCs had the latent ability of migrate to the lesion site of CNV[10]. Therefore, here MSCs was used as systemic delivery vector of siRNA to reach a specific target, which is similar to "Trojan horse" vehicles. This method is also used to improve the delivery of drugs and being engineered with angiogenic, neurotrophic and anti-inflammatory molecules to accelerate the repair of injured or diseased tissues[14]. Stem cells loaded with prodrug-converting enzymes, apoptosis-inducing factors or oncolytic viruses (OVs) have reached clinical trial stage[14]. The use of MSCs as drug carriers has been limited by the poor drug loading capacity, but NPs could increase the drug carrying capacity of MSCs as well as limit their diffusional clearance[12].

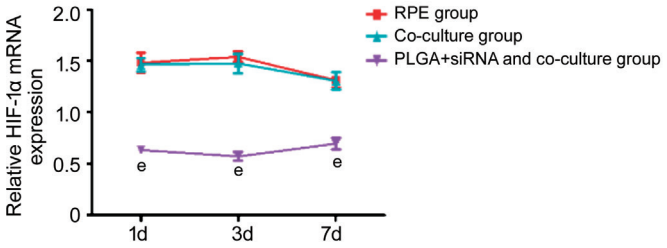


**Figure 11 Effect of mesenchymal stem cells loaded with HIF-1α siRNA nanoparticles on HIF-1α mRNA expression in RPEs under hypoxia model** $^{e}P<0.001$ *vs* RPE group, $n=3$. PLGA: Poly(lactic-co-glycolic acid); HIF-1α: Hypoxia-inducible factor-1α; RPE: Retinal pigment epithelial cells.

MSCs have been engineered with various types of NPs (organic and inorganic matrices) to enhance their drug loading and therapeutic efficacy. PLGA has been approved for human use by FDA and shown immense potential as a good delivery material for a variety of drugs[15]. Generally, nucleic acids are loaded into PLGA NPs by encapsulating them or by adsorption *via* electrostatic attraction between the positively charged surface modification and negatively charged siRNA molecules[16]. PLGA can protect siRNA against RNase enzymatic degradation, and possesses favorable stability to promote safe and sustained release. For sustain release, degradation time of PLGA could be varied from days to

years by regulating the molecular weight and the ratio of its monomers. Cun *et al*[17] incorporated the siRNA in PLGA NPs by using a double emulsion solvent evaporation method, and optimized the formulations of PLGA by varying the siRNA and PLGA ratio which achieved the encapsulation efficiency of more than 70%. In many studies, the size of PLGA NPs prepared by the same method was about 200 nm, and the surface charge was negative[18-19]. In this study, the average diameter of PLGA NPs loaded-HIF siRNA was 314.1 nm but with a rather narrow size distribution, and zeta potential was similar to other studies, showing -0.36 mV. Larger particles have a less burst release than smaller particles, since they have a longer path length of diffusion[20]. And our study showed the PLGA NPs loaded-HIF siRNA can effectively decrease the expression of HIF-1α mRNA by 30%-50% for 7d in RPE cells. SEM imaging revealed that spherical NPs possess a high surface area to volume ratio compared to other shapes (rod, cubic, *etc*.) which produce a more reactive surface and opportunities to therapeutic effects[18]. In the study of transfection of MSCs with PLGA NPs, MSCs demonstrated both concentration and time dependent uptake of NPs, with very little effect on cell viability[21]. Wang *et al*[22] loaded MSC with paclitaxel (Ptx)-PLGA NPs (1 pg/cell Ptx) had little effect on MSC-migration capacity, cell cycle, or multilineage-differentiation potential. Jeon *et al*[23] showed that GFP was expressed by 25.35% of hMSCs transfected with PLGA NP conjugated to polyethylenimine (PEI)/GFP. In this experiment, the transfection efficiency of the PLGA was 67.3%±5.2% by flow cytometry and could be seen around the nucleus of MSCs. Layek *et al*[24] evaluated the MSC-loaded Ptx-PLGA NPs actively homed to the tumor sites and released the drug payload over an extended time.

Due to the existence of blood retinal barrier, this Trojan-horse strategy for retinal diseases therapy employing MSCs transfected with PLGA NPs was here presented. In this experiment, we transfected the PLGA NPs loaded-HIF siRNA into MSCs. The PLGA NPs with sustained-release effect can effectively silence the target gene for a long time to achieve the desired purpose.

RPE cells perform a number of complex functions that are essential for maintenance of the visual function. The abnormal proliferation, migration, and degeneration of RPE cells have an effect on the CNV. In this experiment, RPE cells were co-cultured with MSC-loaded HIF-1α siRNA PLGA NPs in hypoxia model. The results showed that there was no effect of co-culture system on the proliferation, apoptosis, and migration of RPE cells, which showed the presence or absence of MSCs and with or without drug loading had no effect on the proliferation, apoptosis, and migration of RPE cells and partly confirmed safety of the drug delivery system designed in this experiment. In most cases, efficient transfection of ganglion cells can be achieved by intravitreal injections, whereas transfection in the outer retina (photoreceptor and RPE cells) require the more invasive subretinal injection. However, compared to direct injection of NPs, the cells with NPs serving as “Trojan Horse” vehicles could overcome the physiological barriers and exhibit much improved delivery efficiency[25]. It can also reduce the cytotoxicity of direct injection of high concentration NPs to tissues[26].

The expression of HIF-1α mRNA in RPE cells co-cultured with MSC-loaded HIF-1α siRNA PLGA NPs was significantly lower by 40% for 7d. This indicated that this trojan horse biomimetic delivery system could effectively silence the expression of HIF-1α mRNA in RPE cells. In a similar study, in a co-culture system of the melanoma cells and the MSCs loaded with chlorin e6 (Ce6)-conjugated polydopamine nanoparticles (PDA-Ce6), 75% tumor cells caused death even at a low drug loading[13]. Wang *et al*[22] showed that MSCs loaded Ptx could induce tumor cell death *in vitro* and NP-loaded fluorescent MSCs were tracked throughout the tumor mass *in vivo*. Layek *et al*[24] found intravenous injection of nanoparticles resulted in non-specific biodistribution, such as the liver and spleen while nano-engineered MSCs demonstrated selective accumulation and retention in tumors. These studies demonstrate the feasibility of developing nano-engineered MSCs loaded with drugs to improve their targeting or drug resistance properties. Recently, there has also been some evidence that the beneficial effects of MSCs may be achieved by their released extracellular vehicles (EVs)[27-28]. Therefore, to obtain real clinical benefits it is necessary to study the delivery mechanism of NPs in intercellular communication such as exosomes, and gap junctions.

Despite the positive efficacy observed, there are several limitations in this study, which should be addressed in future studies. The effective drug loading and releasing capacity of NPs-MSCs may need to be optimized. Key next steps include release kinetics, safety testing in animals and the delivery mechanism of nanoparticles in intercellular communication. In conclusion, HIF-1α siRNA-NP have been successfully formulated and could enter MSCs. MSCs loaded with HIF-1α siRNA NPs showed desired biological safety and sustained release profiles, which displayed promising therapeutic potential for CNV with potentially reduced injection frequency. Further research is necessary to further explore therapeutic applications of MSCs in patients with CNV.

**ACKNOWLEDGEMENTS**

**Foundations:** Supported by Key Research and Development Program of Shaanxi Province, China (No.2020SF-267); the Natural Science Basis Research Plan in Shaanxi Province of China (No.2022JM-514); Bethune·Lumitin Research

Funding for the Young and Middle-aged Ophthalmologists (No.BJ-LM2021011J); Xi'an Science and Technology Project [No.20YXYJ0008(3)]; Research Incubation Fund of Xi'an People's Hospital (Xi'an Fourth Hospital) (No.ZD-5, ZD-7, and ZD-8).

**Conflicts of Interest: Zhang L,** None; **Yan JJ,** None; **Wang HY,** None; **Li MQ,** None; **Wang XX,** None; **Fan L,** None; **Wang YS,** None.

**REFERENCES**

1 Feng L, Ju M, Lee KYV, Mackey A, Evangelista M, Iwata D, Adamson P, Lashkari K, Foxton R, Shima D, Ng YS. A proinflammatory function of Toll-like receptor 2 in the retinal pigment epithelium as a novel target for reducing choroidal neovascularization in age-related macular degeneration. *Am J Pathol* 2017;187(10):2208-2221.

2 Zhang C, Han M, Wu S. Silencing fibroblast growth factor 7 inhibits krypton laser-induced choroidal neovascularization in a rat model. *J Cell Biochem* 2019;120(8):13792-13801.

3 Plastino F, Santana-Garrido Á, Pesce NA, Aronsson M, Lardner E, Mate A, Kvanta A, Vázquez CM, André H. Echinomycin mitigates ocular angiogenesis by transcriptional inhibition of the hypoxia-inducible factor-1. *Exp Eye Res* 2021;206:108518.

4 Wang LF, Yan ZY, Li YL, Wang YH, Zhang SJ, Jia X, Lu L, Shang YX, Wang X, Li YH, Li SY. Inhibition of Obtusifolin on retinal pigment epithelial cell growth under hypoxia. *Int J Ophthalmol* 2019;12(10):1539-1547.

5 Zhang P, Zhou YD, Tan Y, Gao L. Protective effects of piperine on the retina of mice with streptozotocin-induced diabetes by suppressing HIF-1/VEGFA pathway and promoting PEDF expression. *Int J Ophthalmol* 2021;14(5):656-665.

6 Tai W. Current aspects of siRNA bioconjugate for in vitro and in vivo delivery. *Molecules* 2019;24(12):2211.

7 Serrano-Sevilla I, Artiga Á, Mitchell SG, De Matteis L, de la Fuente JM. Natural polysaccharides for siRNA delivery: nanocarriers based on chitosan, hyaluronic acid, and their derivatives. *Molecules* 2019;24(14):2570.

8 de la Torre P, Pérez-Lorenzo MJ, Alcázar-Garrido Á, Flores AI. Cell-based nanoparticles delivery systems for targeted cancer therapy: lessons from anti-angiogenesis treatments. *Molecules* 2020;25(3):715.

9 Labusca L, Herea DD, Mashayekhi K. Stem cells as delivery vehicles for regenerative medicine-challenges and perspectives. *World J Stem Cells* 2018;10(5):43-56.

10 Hou HY, Liang HL, Wang YS, Zhang ZX, Wang BR, Shi YY, Dong X, Cai Y. A therapeutic strategy for choroidal neovascularization based on recruitment of mesenchymal stem cells to the sites of lesions. *Mol Ther* 2010;18(10):1837-1845.

11 Qiu F, Meng T, Chen Q, Zhou K, Shao Y, Matlock G, Ma X, Wu W, Du Y, Wang X, Deng G, Ma JX, Xu Q. Fenofibrate-loaded biodegradable nanoparticles for the treatment of experimental diabetic retinopathy and neovascular age-related macular degeneration. *Mol Pharm* 2019;16(5):1958-1970.

12 Zhang C, Wang YS, Wu H, Zhang ZX, Cai Y, Hou HY, Zhao W, Yang XM, Ma JX. Inhibitory efficacy of hypoxia-inducible factor 1alpha short hairpin RNA plasmid DNA-loaded poly (D, L-lactide-co-glycolide) nanoparticles on choroidal neovascularization in a laser-induced rat model. *Gene Ther* 2010;17(3):338-351.

13 Ouyang X, Wang X, Kraatz HB, Ahmadi S, Gao J, Lv Y, Sun X, Huang Y. A Trojan horse biomimetic delivery strategy using mesenchymal stem cells for PDT/PTT therapy against lung melanoma metastasis. *Biomater Sci* 2020;8(4):1160-1170.

14 Kimbrel EA, Lanza R. Next-generation stem cells—ushering in a new era of cell-based therapies. *Nat Rev Drug Discov* 2020;19(7):463-479.

15 Matta J, Maalouf R. Delivery of siRNA therapeutics: PLGA nanoparticles approach. *Front Biosci* (*Schol Ed*) 2019;11(1):56-74.

16 Charbe NB, Amnerkar ND, Ramesh B, Tambuwala MM, Bakshi HA, Aljabali AAA, Khadse SC, Satheeshkumar R, Satija S, Metha M, Chellappan DK, Shrivastava G, Gupta G, Negi P, Dua K, Zacconi FC. Small interfering RNA for cancer treatment: overcoming hurdles in delivery. *Acta Pharm Sin B* 2020;10(11):2075-2109.

17 Cun D, Jensen DK, Maltesen MJ, Bunker M, Whiteside P, Scurr D, Foged C, Nielsen HM. High loading efficiency and sustained release of siRNA encapsulated in PLGA nanoparticles: quality by design optimization and characterization. *Eur J Pharm Biopharm* 2011;77(1):26-35.

18 Kelly SJ, Halasz K, Smalling R, Sutariya V. Nanodelivery of doxorubicin for age-related macular degeneration. *Drug Dev Ind Pharm* 2019;45(5):715-723.

19 Noh C, Shin HJ, Lee S, Kim SI, Kim YH, Lee WH, Kim DW, Lee SY, Ko YK. CX3CR1-targeted PLGA nanoparticles reduce microglia activation and pain behavior in rats with spinal nerve ligation. *Int J Mol Sci* 2020;21(10):3469.

20 Ding D, Zhu Q. Recent advances of PLGA micro/nanoparticles for the delivery of biomacromolecular therapeutics. *Mater Sci Eng C Mater Biol Appl* 2018;92:1041-1060.

21 Sadhukha T, O'Brien TD, Prabha S. Nano-engineered mesenchymal stem cells as targeted therapeutic carriers. *J Control Release* 2014;196:243-251.

22 Wang X, Gao J, Ouyang X, Wang J, Sun X, Lv Y. Mesenchymal stem cells loaded with paclitaxel-poly(lactic- co-glycolic acid) nanoparticles for glioma-targeting therapy. *Int J Nanomedicine* 2018;13:5231-5248.

23 Jeon SY, Park JS, Yang HN, Woo DG, Park KH. Co-delivery of SOX9 genes and anti-Cbfa-1 siRNA coated onto PLGA nanoparticles for chondrogenesis of human MSCs. *Biomaterials* 2012;33(17):4413-4423.

24 Layek B, Sadhukha T, Panyam J, Prabha S. Nano-engineered mesenchymal stem cells increase therapeutic efficacy of anticancer drug through true active tumor targeting. *Mol Cancer Ther* 2018;17(6):1196-1206.

25 Li Z, Yu XF, Chu PK. Recent advances in cell-mediated nanomaterial delivery systems for photothermal therapy. *J Mater Chem B* 2018;6(9):1296-1311.

26 Adijanto J, Naash MI. Nanoparticle-based technologies for retinal gene therapy. *Eur J Pharm Biopharm* 2015;95:353-367.

27 Tsiapalis D, O'Driscoll L. Mesenchymal stem cell derived extracellular vesicles for tissue engineering and regenerative medicine applications. *Cells* 2020;9(4):991.

28 He GH, Zhang W, Ma YX, Yang J, Chen L, Song J, Chen S. Mesenchymal stem cells-derived exosomes ameliorate blue light stimulation in retinal pigment epithelium cells and retinal laser injury by VEGF-dependent mechanism. *Int J Ophthalmol* 2018;11(4): 559-566.